26th International Congress of Mechanical Engineering
COBEM 2021
ABCM Associação Brasileira de Engenharia e Ciências Mecânicas
November 22-26, 2021, Virtual Congress, Brazil

COB-2021-0833
A Unified Approach for the Dynamics of Flexible Tethered Wings

Olaf P. V. Pinheiro
olafpalmer@gmail.com
Flávio L. Cardoso-Ribeiro
flaviocr@ita.br
Mauricio A. V. Morales
morales@ita.br
Instituto Tecnológico de Aeronáutica

Abstract. *The Airborne Wind Energy (AWE) is a growing field of research that intends to develop solutions for harvesting wind energy using airborne vehicles. The main advantage of this concept is the capability to explore high altitude winds, which are typically stronger and less variable than in low altitudes. In addition, airborne vehicles tend to require only a fraction of infrastructure costs, when compared with the traditional wind turbines. In the current AWE literature, many modeling strategies for the dynamics of tethered wings are proposed. Important works explored the typical ground generation AWE system with flexible Leading Edge Inflatable (LEI) wings, adopting a variety of combinations of wing structural, aerodynamic and tether models. On the other hand, the studies on flexible aircraft have been a well established subject of research. A useful idea in modeling flexible aircraft is adding the equations of the elastic degrees of freedom (DOFs) in modal coordinates and adopting the mean axis, given the assumption of small displacements. As LEI wings are usually very flexible structures, it emerges an opportunity to apply this same methodology to AWE systems. Additionally, the tether dynamics can be included, taking into account the effects of flexibility, weight distribution and drag forces over the tether. This work proposes an approach that unifies: 1) Flight dynamics, with the classical rigid-body 6 DOFs; 2) Structural dynamics, with wing elastic DOFs in modal coordinates; 3) Tether dynamics, including the DOFs of the flexible tether, as well as the control inputs in the bridle lines; and 4) Quasi-steady aerodynamics, using a Vortex Lattice Method (VLM) implementation, resulting in a seamless integration framework.*

Keywords: *Airborne Wind Energy, Flight Dynamics, Tethered Wings, Kites*

1. INTRODUCTION

In the last two decades, several research groups and startups have been developing concepts of Airborne Wind Energy (AWE), which consists in applications of airborne vehicles to harvest wind energy. Some examples can be mentioned: application of automated controlled kites as auxiliary ship propulsion and wind energy generation (Milanese *et al.*, 2013), (Van der Vlugt *et al.*, 2013) and (Dunker, 2013).

The first relevant theoretical development was introduced by (Loyd, 1980). The entitled *Crosswind Kite Power* analyzed the performance of a C-5A aircraft when attached to the ground by a tether. In AWE systems, a "tethered aircraft" is used to transmit the aerodynamic forces at high altitude winds to an on-ground generator. Alternatively, the electric generator may be embedded as a high altitude wind turbine. (Loyd, 1980) named these two different ways of energy exploitation as *lift mode* and *drag mode*, respectively.

While design concepts, academic works and industrial attention have emerged since early 2000s, many modeling strategies have been studied in order to represent the dynamics of the tethered aircraft. (Gros and DIEHL, 2013) simply added a rigid tether as constraint to the flight dynamics of a rigid aircraft. Moreover, wings made of inflatable structural elements are modeled in (Breukels, 2011) and (Bosch *et al.*, 2013). A typical kite design is illustrated in the figure 1.

In this paper, a generic design of a LEI C-shaped wing is studied. Approaches available in recent and classical works on flexible aircraft literature are applied in this development. The main purpose of this article is to provide a methodology that represents the major phenomena of the LEI wings dynamics such as: the steering control mechanism; aeroelastic effects and the flexible tether dynamics.

This paper is organized as follows: firstly, the equations of motion for flexible aircraft are briefly recalled in Section

2. Secondly, the proposed dynamic model of the tethered wing is described in Section 3. Then, a numerical example considering the computation of equilibrium condition and time-domain simulation is presented in Section 4. Finally, conclusions and further work are discussed in Section 5.

Figure 1: Example of a typical LEI kite. Bosch *et al.* (2013)

2. Flexible Aircraft Equations of Motion

The equations of motion of the flexible aircraft are obtained via Lagrange Equations in (Guimarães Neto, 2014) and (Reschke, 2006). The assumption of small displacements also allows the adoption of the mean axes (Waszak, 1988), which considerably simplifies the equations by removing inertia coupling between rigid body and structural dynamics. The dynamics in the body reference frame are given by the equation 1.

$$\begin{aligned} m\dot{\boldsymbol{V}}_b - m\widetilde{\boldsymbol{s}_{C,b}}\dot{\boldsymbol{\omega}}_b &= \boldsymbol{F}_b^{ext} + m\boldsymbol{g}_b - m\boldsymbol{\omega}_b\boldsymbol{V}_b - m\widetilde{\boldsymbol{\omega}}^2 s_{C,b} \\ m\widetilde{s_C, b}\dot{\boldsymbol{V}}_b + \boldsymbol{J}_{O,b}\dot{\boldsymbol{\omega}}_b &= \boldsymbol{M}_{O,b}{}^{ext} + m\widetilde{\boldsymbol{s}_{C,b}}\boldsymbol{g}_b - m\widetilde{\boldsymbol{s}_{C,b}}\widetilde{\boldsymbol{\omega}_b}\boldsymbol{V}_b - \widetilde{\boldsymbol{\omega}_b}\boldsymbol{J}_{O,b} \\ \boldsymbol{\mu}\ddot{\boldsymbol{\eta}} &= \boldsymbol{\varphi} - \boldsymbol{\kappa}\boldsymbol{\eta} - \boldsymbol{\beta}\dot{\boldsymbol{\eta}} \end{aligned} \tag{1}$$

For an aircraft of mass m, inertia matrix $\boldsymbol{J}_{O,b}$, center of mass coordinates $\boldsymbol{s}_{C,b}$, modal mass matrix $\boldsymbol{\mu}$, modal stiffness matrix $\boldsymbol{\kappa}$ and modal damping matrix $\boldsymbol{\beta}$. $\boldsymbol{V}_b$ and $\boldsymbol{\omega}_b$ are the linear and angular velocities, respectively. $\boldsymbol{\eta}$ represents the elastic DOFs of the aircraft in the modal coordinates. Finally, $\boldsymbol{F}_b^{ext}$ and $\boldsymbol{M}_{O,b}{}^{ext}$ are the external forces and moments and $\boldsymbol{\varphi}$ is the generalized modal force. The quantities are given in the body coordinate system.

Using the conventional Euler angles for roll, pitch and yaw, (ϕ, θ, ψ), the rotation matrices are:

$$\boldsymbol{R}_1(\phi) = \begin{bmatrix} 1 & 0 & 0 \\ 0 & \cos\phi & \sin\phi \\ 0 & -\sin\phi & \cos\phi \end{bmatrix}, \boldsymbol{R}_2(\theta) = \begin{bmatrix} \cos\theta & 0 & -\sin\theta \\ 0 & 1 & 0 \\ \sin\theta & 0 & \cos\theta \end{bmatrix}, \boldsymbol{R}_3(\psi) = \begin{bmatrix} \cos\psi & \sin\psi & 0 \\ -\sin\psi & \cos\psi & 0 \\ 0 & 0 & 1 \end{bmatrix}$$

Therefore, the transformation matrix from the inertial coordinate system (v) to the body coordinate system (b) is given by: $\boldsymbol{R}_{b/v} = \boldsymbol{R}_1(\phi)\,\boldsymbol{R}_2(\theta)\,\boldsymbol{R}_3(\psi)$ and, inversely: $\boldsymbol{R}_{v/b} = \boldsymbol{R}_{b/v}^T$

The rotational kinematics can be expressed by the equation 2:

$$\dot{\boldsymbol{\Theta}} = \boldsymbol{K}(\boldsymbol{\Theta})^{-1}\boldsymbol{\omega}_b \tag{2}$$

where: $\boldsymbol{K}(\boldsymbol{\Theta}) = \begin{bmatrix} 1 & 0 & -\sin\theta \\ 0 & \cos\phi & \sin\phi\cos\theta \\ 0 & -\sin\phi & \cos\phi\cos\theta \end{bmatrix}, \boldsymbol{\Theta} = \begin{bmatrix} \phi \\ \theta \\ \psi \end{bmatrix}$

At last, the translation kinematics is described by the equation 3, where x, y are the coordinates in the inertial frame and h is the altitude.

$$\begin{bmatrix} \dot{x} \\ \dot{y} \\ -\dot{h} \end{bmatrix} = \boldsymbol{R}_{v/b}\boldsymbol{V}_b \tag{3}$$

For the kite model studied in this work, the same equations of motion (1, 2 and 3) are applied, considering that the envelope of operation in this analysis is such that the assumption of small displacements is satisfied.

3. Dynamic Model for Flexible Tethered Wing

In this section, the aeroelastic model for a flexible tethered wing is described. Firstly, the structural model for the kite, obtained using finite elements is presented in the section § 3.1. Secondly, the aerodynamic model is presented in the section § 3.2. Finally, the tether model is described in § 3.3.

3.1 Structural Model

LEI wings can be idealized as a set of special beams, whose properties were experimentally obtained in Breukels (2011). The author fits a set of tip forces and torsion functions, varying with the diameter, d, internal pressure p, and the structural displacement, w, or twist, ϑ, as illustrated in the figure 3. In the figure 2, a scheme of a inflatable beam element is shown.

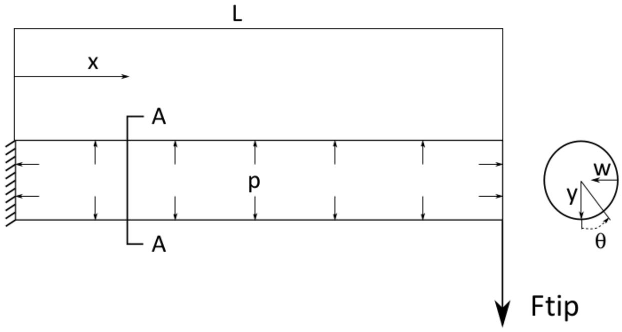

Figure 2: Inflatable beam element. (Schwoll, 2012)

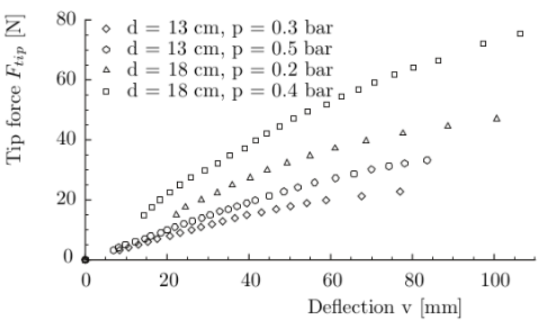

(a) Deflection curves in bending.

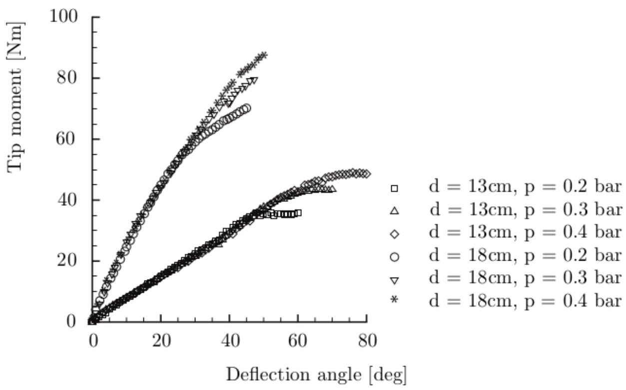

(b) Twisting curves in torsion.

Figure 3: Experimental data of the structural properties of inflatable beams. (Breukels, 2011)

Assuming small displacements, the empirical curves presented in Breukels (2011) for tip force $F_{tip}(p, d, w)$ and torsion $T(p, d, \vartheta)$ can be linearized around zero.

$$F_{tip} = \left(\frac{\partial F_{tip}}{\partial w} \Big|_{w=0} \right) w$$

$$T = \left(\frac{\partial T}{\partial \vartheta} \Big|_{\vartheta=0} \right) \vartheta$$

The derivatives $\frac{\partial F_{tip}}{\partial w}\Big|_{w=0}$ and $\frac{\partial T}{\partial \vartheta}\Big|_{\vartheta=0}$ depend only on pressure and diameter. Given the expressions for bending and torsion rigidities: $(EI) = \frac{FL^3}{3w}$ and $(GJ) = \frac{TL}{\vartheta}$, where L is the length of the beam, it yields to:

$$(EI) = \left(\frac{\partial F_{tip}}{\partial w} \Big|_{w=0} \right) \frac{L^3}{3}$$

$$(GJ) = \left(\frac{\partial T}{\partial \vartheta} \Big|_{\vartheta=0} \right) L$$

LEI kites are usually made of a combination of plastic materials, namely: Dacron, ripstop Nylon and thermoplastic polyurethane. Their properties can be obtained from (Schwoll, 2012). Then, the inflatable beams can be represented by CBARs NASTRAN elements, applied for Leading Edge and Struts. Trailing Edge and Wingtips are wires which are also represented by CBAR elements. The structural model is illustrated in the figure 4a.

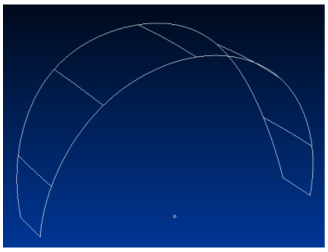

(a) LEI wing NASTRAN model using CBAR elements.

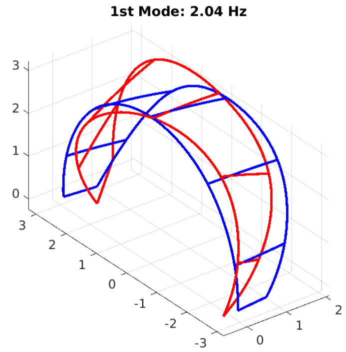

(b) 1st mode.

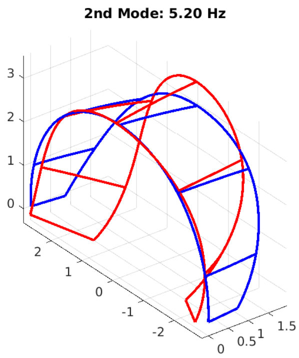

(c) 2nd mode.

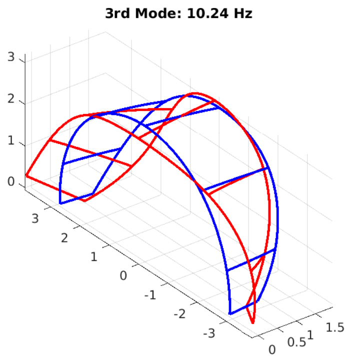

(d) 3rd mode.

Figure 4: Vibration modes of the kite.

From NASTRAN 103 solution, modal matrix Φ, mass matrix M, stiffness matrix K are obtained. Retaining only the first n_r eigenvectors, the modal matrices to be used in the equations of motion are:

$$\begin{aligned} \boldsymbol{\kappa} &= \Phi_r^T K \Phi_r \\ \boldsymbol{\mu} &= \Phi_r^T M \Phi_r \end{aligned} \tag{4}$$

In the ref. (Bosch *et al.*, 2013), the structural model also considers membrane elements in order to assess the displacements in the wing stations and carry the aerodynamic forces into the beam elements.
For the sake of simplicity, an interpolation scheme is used instead. It consists in finding a mapping matrix M_u that relates the displacements from the structural frame from the vortex-lattice panels.

$$\boldsymbol{u}_{VLM} = M_u \boldsymbol{u}_{frame}$$

3.2 Quasi-Steady Aerodynamic Model

A Vortex-Lattice Method (VLM) implementation is used in order to provide the aerodynamic force distributions and capture local effects of flexibility in the aerodynamics. The pressure differential in the VLM panel is given by:

$$\Delta Cp = Aw$$

where, A is the matrix with the Aerodynamic Influence Coefficients and w is the normalwash of each panel. The method is described by (Hedman, 1966). The flexibility affects the aerodynamic forces by means of the local variation of w. The parasite drag is taken into account using empirical formulas from (Breukels, 2011), based on a CFD database of the typical LEI wing section for different cambers.
Considering each row of chordwise vortex-lattice panel as an independent section, the influence of local parasite drag can be added to the wing. The variations of camber and panel incidences due to flexibility are also taken into account in this implementation.

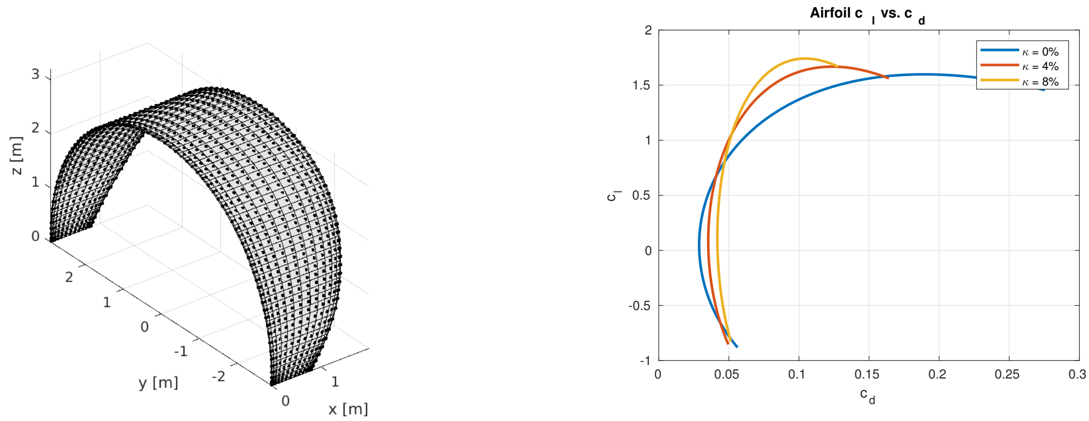

(a) Vortex Lattice model and control points.

(b) Airfoil drag polar based on (Breukels, 2011)

Figure 5: Aerodynamic model.

3.3 Tether Model

Fechner *et al.* (2015) presents a simplified tether model, idealized as a set of bar elements with variable length. The same methodology is adopted and the equations of the tether DOFs are coupled with the flexible wing dynamics. This approach also takes into account the effects of drag and weight distribution on the tether.

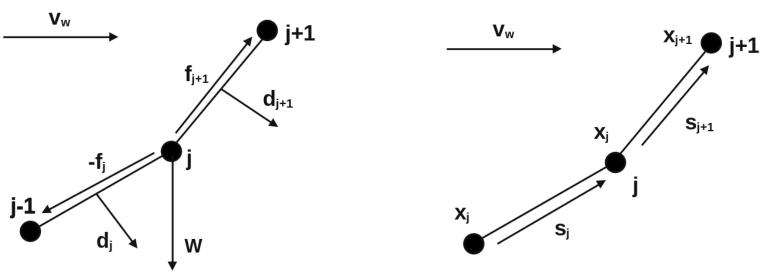

Figure 6: Scheme of the internal forces between tether nodes.

In addition, the bridles are also represented in the tether dynamics. In the junction between bridles and the main tether, it is placed the Kite Control Unit (KCU), which contains the on-board control system of the kite. The equations for each node of the tether and bridles are represented below:

$$\begin{aligned} \dot{x}_{T,j} &= V_{T,j} \\ \dot{V}_{T,j} &= \frac{1}{m_j}\left(-f_j + f_{j+1} + \frac{1}{2}(d_j + d_{j+1})\right) + g \end{aligned} \tag{5}$$

where, $x_{T,j}$ and $V_{T,j}$ are the position and velocity of the j-th tether node, f_j the elastic and damping forces and d_j the drag force on the tether element, as show in the scheme of the figure 7. For the tether segments attached to the trailing edge of the kite, the length are variable in order to provide the steering control of the kite.

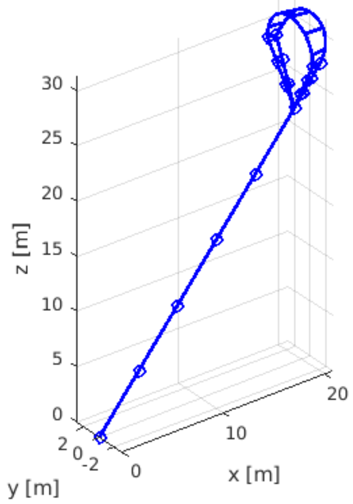

Figure 7: Tether attached to the kite .

4. Numerical Example

In this section, some numerical results of the kite model are presented. The atmospheric model is described in the section § 4.1, the equilibrium calculation is analyzed in the section § 4.2, and lastly, the responses of the modal coordinates to a commanded input is shown in § 4.3.

4.1 Atmospheric model

Tether elements and the kite are subject to a variable wind speed profile. The following logarithmic law for the wind speed is applied (Fechner *et al.*, 2015).

$$v_{w,log} = v_{w,ref} \frac{\log(z/z_0)}{\log(z_{ref}/z_0)} \tag{6}$$

where z_{ref} is the reference height, $v_{w,ref}$ is the ground speed and z_0 is the roughness length.

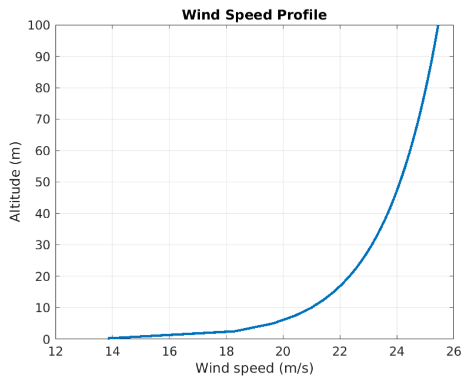

Figure 8: Wind profile.

4.2 Equilibrium condition

Solving the equilibrium problem required an iterative process separating the DOFs of the kite and bridles from the tether and KCU. Once the equilibrium is found, the complete dynamics can be integrated in time. The figures 9a and 9b are representations of an arbitrary step of the equilibrium solution. The figure 10 shows the final equilibrium condition for the kite structure and the tether nodes positions.

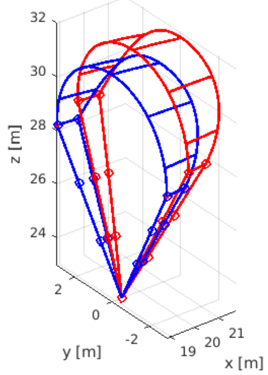

(a) Deformed shape of kite and bridle.

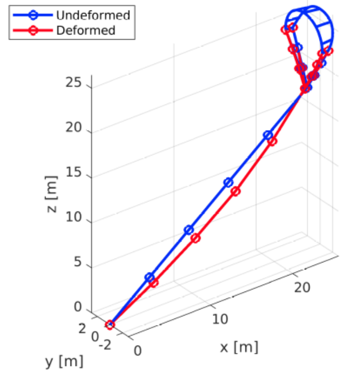

(b) Deformed shape of the tether

Figure 9: Equilibrium for tether, kite and bridles.

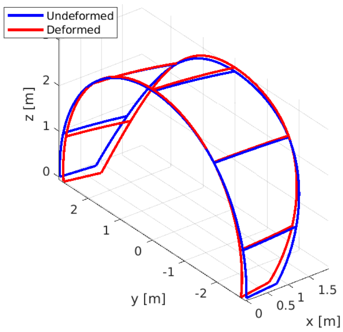

(a) Wing deformed shape in the body system.

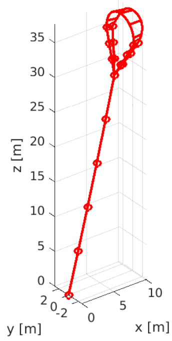

(b) Equilibrium position

Figure 10: Equilibrium Calculation.

4.3 Simulation

From the equilibrium of only the kite-bridle system, the steering command can be demonstrated simulating an input in the steering lines. The results show that the steering mechanism is a direct control of the first mode of the kite. The figure 11b shows that when the steering lines are inversely commanded, the value of η_1 is highly correlated with the input signal. The figure 12 shows some relevant outputs of the simulation.

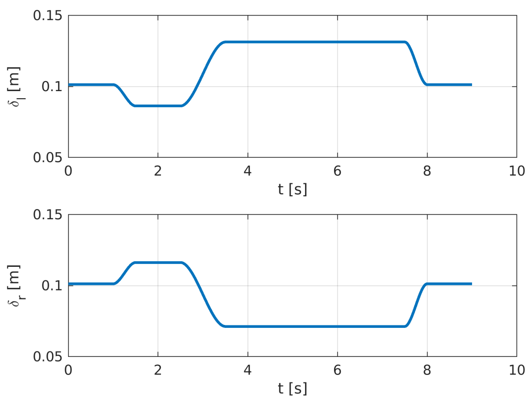

(a) Input. δ is the length added to the steering line.

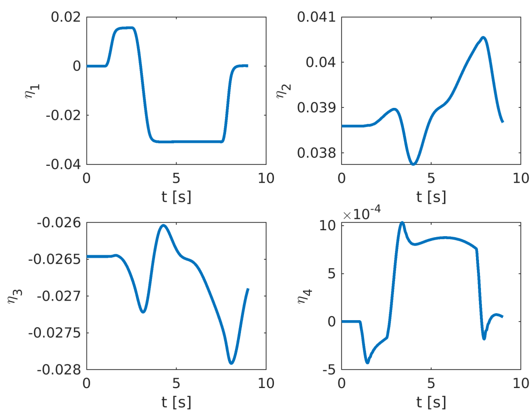

(b) Modal coordinates response

Figure 11: Simulation of a steering line command.

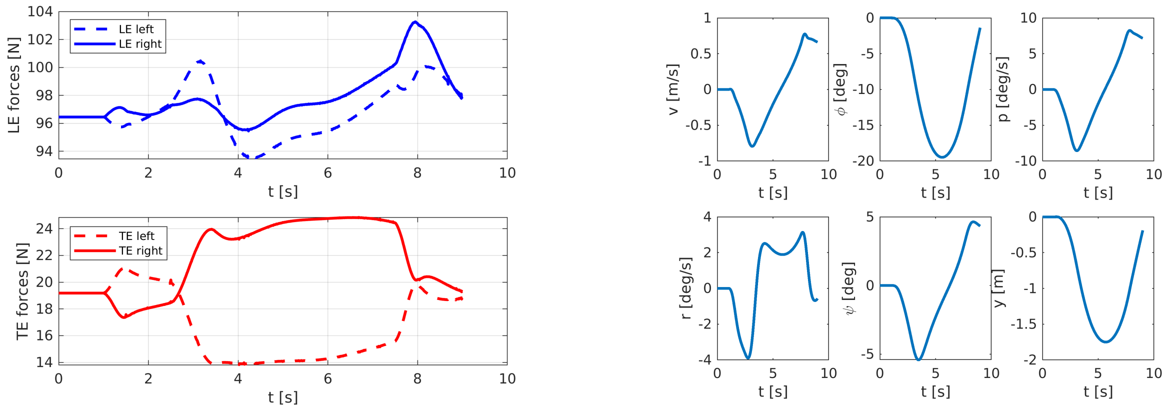

(a) Force outputs at the Leading and Trailing Edge attachments.

(b) Lateral-directional states.

Figure 12: Some relevant outputs of the simulation.

5. Conclusions and Further Work

This paper presented an approach for the dynamics of LEI wings which considered: (1) a structural model based on finite elements, (2) a quasi-steady aerodynamic model using a vortex-lattice method implementation and 3) a flexible tether model. The complete system is subjected to a typical wind profile. The result is a seamless integration framework that is suitable to be applied to AWE systems.

Next steps and further relevant developments may include (1) analysis of response to different command inputs and gusts, (2) addition of electrical generator dynamics and (3) implementation of a flight path tracking and winch control.

6. REFERENCES

Bosch, A., Schmehl, R., Tiso, P. and Rixen, D., 2013. "Nonlinear aeroelasticity, flight dynamics and control of a flexible membrane traction kite." *Airborne Wind Energy, Chapter 17, Springer*.

Breukels, J., 2011. *An Engineering Methodology for Kite Design*. Ph.D. thesis, Ph.D. Thesis in Aerospace Engineering, Delft University of Technology. URL `http://resolver.tudelft.nl/uuid:cdece38a-1f13-47cc-b277-ed64fdda7cdf`.

Dunker, S., 2013. "Ram-air wing design considerations for airborne wind energy." *Airborne Wind Energy*, Vol. Chapter 31.

Fechner, U., Van der Vlugt, R., Schreuder, E. and Schmehl, R., 2015. "Dynamic model of a pumping kite power system". *Renewable Energy*, Vol. 83, pp. 705–716. ISSN 0960-1481. doi:https://doi.org/10.1016/j.renene.2015.04.028. URL `https://www.sciencedirect.com/science/article/pii/S0960148115003080`.

Gros, S. and DIEHL, M., 2013. *Modeling of Airborne Wind Energy Systems in Natural Coordinates*, Springer Berlin Heidelberg, Berlin, Heidelberg, pp. 181–203.

Guimarães Neto, A.B., 2014. *Flight dynamics of flexible aircraft using general body axes: a theoretical and computational study*. Ph.D. thesis, Thesis of Doctor in Science in Flight Mechanics – Instituto Tecnológico de Aeronáutica, São José dos Campos.

Hedman, S.G., 1966. "Vortex lattice method for calculation of quasi steady state loadings on thin elastic wings." *Stockholm: Aeronautical Research Institute of Sweden*.

Loyd, M.L., 1980. "Crosswind kite power (for large-scale wind power production)". *Journal of Energy*, Vol. 4, No. 3, pp. 106–111.

Milanese, M., Taddei, F. and Milanese, S., 2013. "Design and testing of a 60 kw yo-yo airborne wind energy generator." *Airborne Wind Energy*, Vol. Chapter 21.

Reschke, C., 2006. *Integrated Flight Loads Modelling and Analysis for Flexible Transport Aircraft*. Ph.D. thesis, Dissertation (Doctoral Degree) - Institut Flugmechanik und Flugregelung der Universitat Stuttgart, Stuttgart.

Schwoll, J., 2012. *Finite Element Analysis of Inflatable Structures Using Uniform Pressure*. Master's thesis, Master of Science in Aerospace Engineering, Delft University of Technology.

Van der Vlugt, R., Peschel, J. and Schmehl, R., 2013. "Design and experimental characterization of a pumping kite power system." *Airborne Wind Energy*, Vol. Chapter 23.

Waszak, M. R.; Schmidt, D.K., 1988. "Flight dynamics of aeroelastic vehicles." *Journal of Aircraft*, Vol. 25, No. 6, pp. 563–571.

7. RESPONSIBILITY NOTICE

The authors are solely responsible for the printed material included in this paper.